energies

MDPI

Article

Optimization-Based Control Concept with Feed-in and Demand Peak Shaving for a PV Battery Heat Pump Heat Storage System

Ronny Gelleschus *, Michael Böttiger and Thilo Bocklisch

Chair of Energy Storage Systems, Technische Universität Dresden, Helmholtzstr. 9, 01062 Dresden, Germany; michael.boettiger@tu-dresden.de (M.B.); thilo.bocklisch@tu-dresden.de (T.B.)

* Correspondence: ronny.gelleschus@tu-dresden.de; Tel.: +49-351-463-40332

Received: 18 April 2019; Accepted: 22 May 2019; Published: 1 June 2019

Abstract: The increasing share of renewable energies in the electricity sector promotes a more decentralized energy supply and the introduction of new flexibility options. These flexibility options provide degrees of freedom that should be used optimally. Therefore, in this paper, a model predictive control-based multi-objective optimizing energy management concept for a hybrid energy storage system, consisting of a photovoltaics (PV) plant, a battery, and a combined heat pump/heat storage device is presented. The concept's objectives are minimal operation costs and reducing the power exchanged with the electrical grid while ensuring user comfort. In order to prove the concept to be viable and its objectives being fulfilled, investigations based on simulations of one year of operation have been carried out. Comparisons to a simple rule-based strategy and the same model predictive control scheme with ideal forecasts prove the concept's viability while showing improvement potential in the treatment of nonlinear system behavior, caused by nonlinear battery losses, and of forecast uncertainties.

Keywords: energy management; hybrid energy storage system; battery; heat storage; photovoltaics; heat pump; model predictive control; multi-objective optimization

1. Introduction

The global renewable generation capacity is increasing rapidly with the highest growth rates, above 30% from 2016 to 2017 [1], being observed in photovoltaics (PV). Therefore, in the future, not only the consumption, but also the generation of electricity will be fluctuating. Hence, flexibility options are needed in order to ensure a continuing high availability and quality of the energy supply [2]. Two of the most commonly cited flexibility options are energy storage devices and sector coupling. In addition to an increase in the need of flexibility options, the transition to renewable energies also leads to a more decentralized energy system. This often takes the form of prosumers, formerly only energy consumers who upgrade their home with generation facilities. Common domestic generation facilities include PV for electricity production and heat pumps to ensure heat and domestic hot water (DHW) supply. In order to increase self-sufficiency, and therefore reduce energy costs, PV home systems are often equipped with a battery, in most cases based on the lithium-ion technology. Heat pumps are usually coupled with a heat storage device [3–5] or use the building mass as energy storage [6]. Therefore, they are a typical example of flexible sector coupling. A system containing both a battery and heat storage constitutes a hybrid energy storage system [7–9].

Due to the grid usually providing the prosumer's home with a stable AC voltage, the flexibility provided by the battery and the heat pump are degrees of freedom. This means that a control system managing the individual power flows is needed. In practice, these control systems can be divided into

two groups, rule-based and optimization-based concepts [7]. The simplest approach that has previously been implemented in real systems is a rule-based concept for self-consumption optimization, which simply charges the storage device when there is a PV power surplus and discharges the storage device when the load power is higher [4,5,10,11]. On sunny days, this often leads to the storage device being fully charged very early. If there is no feed-in limit, the power fed into the grid changes drastically from zero to about nominal PV power, potentially presenting a problem for the grid operator. If there is a feed-in limit (e.g., in Germany), the PV power is curtailed, which reduces the income of the PV system owner. Therefore, more intelligent rule-based approaches have been reported [12–14] and are already being sold by the industry. However, even if they reach near-optimal performance in cost reduction, they are typically designed for specific system setups and may be difficult to adapt to other systems, other climates, or a changing socio-economic environment such as flexible electricity prices or the emergence of local electricity or grid service markets. Recent research in rule-based concepts tries to address that problem using machine learning to approximate an optimal policy [15].

Optimization-based control systems are a very diverse field of research and can be further divided into categories based on the time of use of optimization. Optimization-based methods may be used offline to calculate optimal rules for a specific system [8,16], but similar to intelligent rule-based approaches, it might be hard or impossible to adapt the same procedure to another, more complex system. Optimization may also be used as a day-ahead planning tool in order to calculate optimal power and energy trajectories based on PV and load forecasts [17–19]. However, as forecasts are never perfectly correct, some error correction mechanism has to be implemented or performance may be very poor. Finally, there is the possibility of using model predictive control (MPC), which re-evaluates the optimization problem in regular intervals in order to correct for forecast errors [5,6,11,19–25].

These MPC-based energy management concepts usually show a very good performance in reaching their respective objectives. A very simple linear programming formulation for a PV battery system was used in [11] in order to not only minimize costs almost as well as in the rule-based self-consumption optimization concept, but also reduce PV curtailment and smoothen the power fed into the grid. The authors of [19] studied the advantages of an MPC scheme compared to day-ahead scheduling for the energy cost reduction of a PV battery system with time-of-use tariffs. However, the nonlinear behavior of batteries was not taken into account in the simulations of both papers. In [6], a linear programming-based MPC scheme for space heating with a heat pump was used for operation cost minimization by taking advantage of flexible electricity tariffs using the thermal storage capacity of the building. A stochastic mixed-integer linear programming (MILP) formulation was used in [20] to minimize operation cost and local CO2 emissions in a local microgrid. The authors of [5] propose a nonlinear optimization-based distributed MPC scheme for a hybrid energy storage system consisting of a battery and two hot water storages with a PV system and an air-source heat pump. By using forecasts for the outside temperature and PV production, and the flexibility provided by the storages, the heat pump could be operated at times with higher source temperature and PV availability. This increases both the heat pump's coefficient of performance (COP) and the renewable energy coverage, and therefore, saves money. In [21], a multi-stage stochastic MPC concept for a PV battery system is proposed. It is shown that through the use of dynamic programming, which allows fast nonlinear optimization for small-scale systems and for modeling the uncertainties in the PV and load forecasts, significantly better results in terms of energy cost reduction can be obtained. As including the uncertainties in an optimization model increases the calculation times, approximations of the stochastic cost function [22,23] or, in the case of dynamic programming, the value function [22,24] can be used.

In all these cases, MPC was used to save money to the sole advantage of the owner of the storage system. In many situations, this does not use the storages devices' flexibility to the full extent. Therefore, with fitting incentives for the storage system owners, these systems can additionally benefit other market participants, e.g., by lowering the grid load and thereby deferring or averting the need for grid reinforcements. Therefore, the inclusion of more objectives, like smoothing the grid power or increasing the devices' lifetimes, seems desirable. In [25], a multi-objective MPC scheme for a PV battery system

using dynamic programming is presented. The objectives include minimizing costs and smoothing both grid feed-in and import power, as well as increasing the lifetime of the battery. However, because of the so-called "curse of dimensionality", the calculation time of dynamic programming increases progressively with the number of possible system states, which is disadvantageous for the application of MPC in systems with many storage devices [26].

This paper presents a novel multi-objective home energy management concept using MILP and MPC that reduces energy costs as well as the maximum grid loads both on feed-in and demand sides. It operates on a grid-coupled home energy system with a PV plant, a battery and a combined heat pump/heat storage device for DHW supply. A simulation model for that system is presented in Section 2. The energy management concept is explained in Section 3. Section 4 presents a comparison between the new energy management concept and a classical rule-based self-consumption scheme, both qualitatively on the basis of power and energy trajectories on a time span of several days, as well as quantitatively based on a simulation of a one-year operation. Further improvement potentials for the new concept are evaluated by comparing its performance using real and ideal forecasts. Finally, in Section 5, conclusions are drawn and an outlook on further research is given.

2. Simulation Model

The system to be controlled consists of a PV plant, a battery, a combined heat pump/heat storage device for DHW supply, household loads, and a connection to the public electricity grid. An overview is shown in Figure 1.

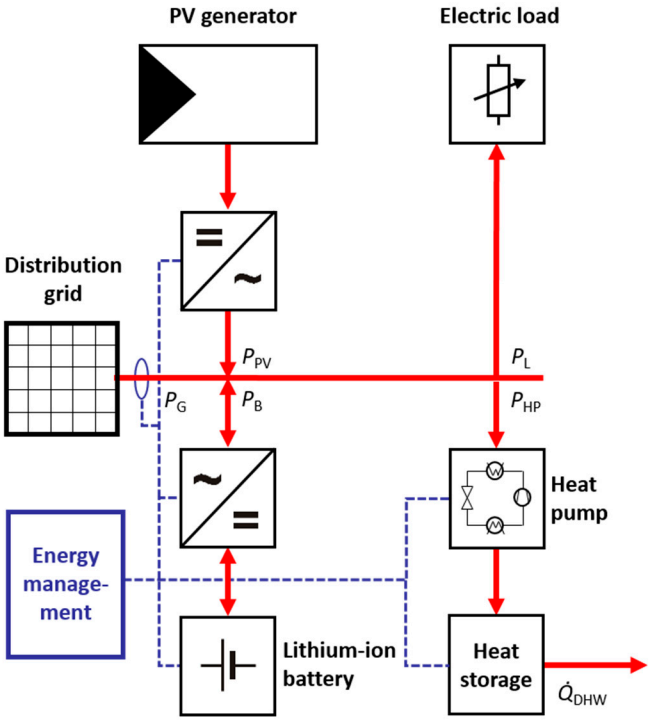

Figure 1. The photovoltaics (PV) battery heat pump heat storage system to be controlled. Red lines: power flows (electrical and thermal). Blue lines: information flows.

2.1. Battery Model

The battery is modeled using a look-up table based on measurements of a real battery. First, the battery was charged and discharged with different currents. Then, based on the measurements, an equivalent circuit-based model was parameterized. This procedure is explained extensively in [27]. As such a model is better used for transient analyses on a millisecond to second scale and the available PV and load data have a one-minute resolution, a further abstraction was carried out, by simulating

constant charge or discharge currents for different starting states of charge (SOC) over one minute and filling a look-up table with the resulting average losses, including inverter losses. The result is illustrated in Figure 2a.

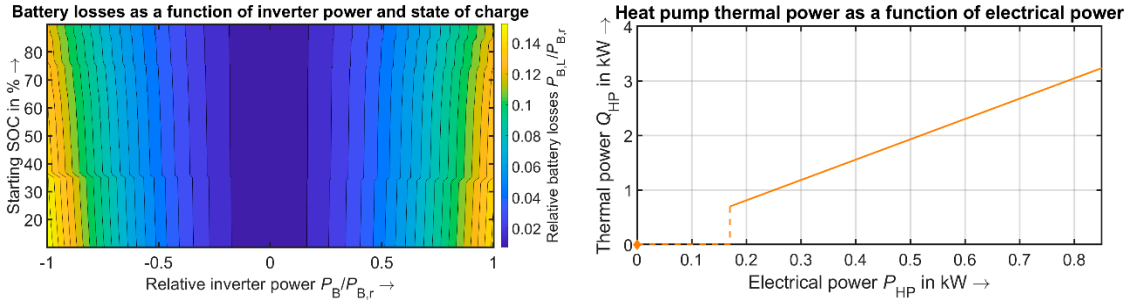

(**a**) (**b**)

Figure 2. (**a**) Battery losses in relation to rated inverter power as a function of relative inverter power and current state of charge (SOC). (**b**) Heat pump thermal power as a function of electrical power.

Using these losses $P_{B,L}$ from the look-up table, the battery's energy content E_B in time step k is calculated using the time step size Δt and battery power P_B as:

$$E_B(k) = E_B(k-1) + \Delta t \cdot (P_B(k) - P_{B,L}(k)). \tag{1}$$

2.2. Heat Pump/Heat Storage Model

The heat pump/heat storage device model uses the same look-up table structure as the battery. According to [28], inverter-driven heat pumps have a higher COP during partial load operation. Therefore, as a very simple model for presenting the new control scheme, a linear behavior with the rated COP at full load and a slightly higher COP at 20 % partial load as supporting points is assumed. The heat pump has to be either switched off or switched on with a power P_{HP} between 20% and 100% of the rated power. The resulting characteristic curve is shown in Figure 2b.

Using the resulting thermal power $\dot{Q}_{HP}$ and the enthalpy flow of the hot water being drawn, $\dot{Q}_{DHW}$, the heat content U of the heat storage is calculated as:

$$U(k) = U(k-1) + \Delta t \cdot \left(\dot{Q}_{HP}(k) - \dot{Q}_{DHW}(k) - R_{TH,SD}(k)\right), \tag{2}$$

with the rate of self-discharge over the storage walls:

$$R_{TH,SD}(k) = k_{th} \cdot A \cdot \left(\frac{U(k-1)}{m_{H_2O} \cdot c_p} - (T_a - T_{ref})\right), \tag{3}$$

where k_{th} is the thermal transmittance of the storage walls, A is the storage surface, T_a is the ambient temperature, T_{ref} is the reference temperature (at which $U = 0$), m_{H_2O} is the mass of the storage's water content, and c_p its specific heat capacity.

2.3. PV Plant, Electrical Load, Heat Load

The PV plant and the household loads are modeled by directly using rescaled measured time series of the AC powers from a four-person household in Chemnitz, Germany, with the additional possibility of curtailing PV power. The heat load is a stochastically generated time series for a four-person household from the tool described in [29]. All three time series have a one-minute resolution.

2.4. Grid Model

The grid power is calculated from the sum of all other electric powers in the system. Independently of the energy management concept, a strict feed-in limit $P_{G,max}$ of 50% of the PV rated power has to be met. Therefore, after the energy management concept calculated the battery and heat pump powers, the curtailment and grid powers $P_{PV,ct}$ and P_G are calculated using the load and maximum possible PV powers P_L and P_{PV} as:

$$P_{diff} = P_{PV} - P_B - P_L - P_{HP}, \tag{4}$$

$$P_{PV,ct} = \max(0, P_{diff} - P_{G,max}), \tag{5}$$

$$P_G = P_{diff} - P_{PV,ct}. \tag{6}$$

3. Energy Management Concept

3.1. Control Structure

The energy management concept aims to simultaneously reduce operation cost and peak powers in grid import and grid export, while ensuring a high quality of service for the DHW supply. The combination of these goals can be formulated as an optimization problem. Therefore, the energy management concept is based on the MPC framework.

Due to the high computational effort involved in optimizing this system, in a real setup with a microcontroller the optimization can only be carried out every few minutes. Therefore, in order to ensure the grid power reduction on a short timescale, the control concept is enhanced with an additional inner control loop which controls the grid power by adapting battery power. For the purpose of the simulations reported in the next section, a perfect performance of this inner control loop is assumed. The control structure is shown in Figure 3.

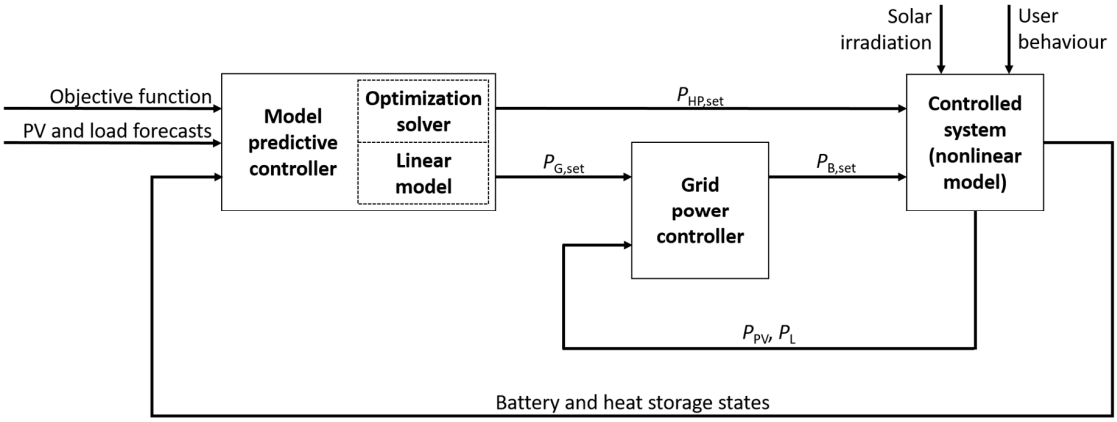

Figure 3. Structure of the suggested control approach: The (nonlinear) system is controlled by a linear optimization-based model predictive controller with an inner control loop.

3.2. PV and Load Forecasts

The forecasts use simple heuristics. The PV and electical load forecasts are identical to those in [30]. In order to obtain the PV forecast, firstly, the envelope of the PV powers $P_{PV,env}$ of the previous 10 days is calculated. Secondly, based on the previous three hours, a clear sky index (CSI) is calculated as:

$$CSI = \frac{\int_{t_0-3h}^{t_0} P_{PV}(t)\,\mathrm{d}t}{\int_{t_0-3h}^{t_0} P_{PV,env}(t)\,\mathrm{d}t}. \tag{7}$$

Finally, the forecasted PV power for all time steps is the CSI multiplied with the envelope for the respective time step. The electrical load forecast is calculated as a weighted average of an instantaneous

and a daily persistence, with the weight w of the instantaneous persistence decreasing exponentially over the prediction horizon:

$$w(k) = \exp(0.1 \cdot (1-k)), \tag{8}$$

$$P_{\mathrm{L,f}}(k) = w(k) \cdot P_{\mathrm{L}}(0) + (1-w(k)) \cdot P_{\mathrm{L}}\left(-\frac{24\,\mathrm{h}}{\Delta t} + k\right), \tag{9}$$

where 0 means the current time step and k the time step that we want to predict.

The DHW demand consists of many discrete events which are difficult to predict exactly. However, due to most people having recurring habits, persistence forecasts usually provide acceptable results. In order to compensate for slightly varying behavior, e.g., a person showering a bit earlier in the morning, the forecast is constructed from the time series of the preceding day, moved half an hour earlier.

3.3. Optimization Problem Formulation

In order to implement an MPC, an optimization formulation of the system to be controlled is needed. This includes a description of the physical system and its socio-economic environment, as well as an objective function. The following paragraphs show that most terms involved in this description are linear, with the exception of both energy storage balances. However, assuming constant battery efficiencies and heat pump COPs, which is done quite regularly (see e.g., [3,11,20]), makes the problem to be solved a MILP. For this kind of problem very efficient solvers are available both freely (e.g., the open-source COIN-OR Branch & Cut, CBC) and commercially (e.g., IBM ILOG CPLEX).

The main control objectives are lowering the operation costs C of the system and relieving the electric distribution grid of stress in the form of peak powers $P_{\mathrm{G,B,max}}$ and $P_{\mathrm{G,FI,max}}$. The high quality of service for the DHW supply is ensured by introducing a penalty term F_{thermal}. These objectives translate into four linear terms that can be linearly combined into one objective function F with weights α, β and γ:

$$\text{minimize } F = C + \alpha \cdot P_{\mathrm{G,B,max}} + \beta \cdot P_{\mathrm{G,FI,max}} + \gamma \cdot F_{\mathrm{thermal}}, \tag{10}$$

where:

$$C = \sum\nolimits_{k=1}^{K} p_{\mathrm{G,B}}(k) \cdot P_{\mathrm{G,B}}(k) \cdot \Delta t - p_{\mathrm{G,FI}}(k) \cdot P_{\mathrm{G,FI}}(k) \cdot \Delta t, \tag{11}$$

$$P_{\mathrm{G,B}}(k) \leq P_{\mathrm{G,B,max}} \ \forall k, \tag{12}$$

$$P_{\mathrm{G,FI}}(k) \leq P_{\mathrm{G,FI,max}} \ \forall k, \tag{13}$$

$$F_{\mathrm{thermal}} = \sum\nolimits_{k=1}^{K} U_{\mathrm{penalty}}(k) \cdot \Delta t, \tag{14}$$

$$U(k) + U_{\mathrm{penalty}}(k) \geq U_{\mathrm{min}} \ \forall k. \tag{15}$$

k is the index of a time step in the future, K is the number of time steps in the prediction horizon, Δt is the optimization time step size, which is equal to the adaptation interval, $p_{\mathrm{G,B}}$ and $p_{\mathrm{G,FI}}$ are the electricity price and feed-in tariffs, respectively, and $P_{\mathrm{G,B}}$ and $P_{\mathrm{G,FI}}$ are the grid import and feed-in powers. U is the usable energy content of the hot water storage and U_{penalty} is an auxiliary variable denoting the amount of energy that the heat storage is short of for a user-specified minimum U_{min}, indicating a too low water temperature.

Any solution to the optimization problem needs to fulfill three energy balances. These are the battery energy balance, the heat storage energy balance and the electrical power balance. The battery energy balance relates the change of stored energy E_{B} to the charging and discharging powers $P_{\mathrm{B,C}}$ and $P_{\mathrm{B,D}}$ and the self-discharge rate $R_{\mathrm{B,SD}}$, taking into account charging and discharging efficiencies η_{C} and η_{D}:

$$\frac{E_{\mathrm{B}}(k) - E_{\mathrm{B}}(k-1)}{\Delta t} = \eta_{\mathrm{C}} \cdot P_{\mathrm{B,C}}(k) - \frac{P_{\mathrm{B,D}}(k)}{\eta_{\mathrm{D}}} - R_{\mathrm{B,SD}} \ \forall k. \tag{16}$$

The heat storage balance is described by:

$$\frac{U(k) - U(k-1)}{\Delta t} = \epsilon_{\mathrm{COP}} \cdot P_{\mathrm{HP}}(k) - \dot{Q}_{\mathrm{DHW}}(k) - R_{\mathrm{TH,SD}} \; \forall k, \tag{17}$$

where ϵ_{COP} is the COP of the heat pump and $R_{\mathrm{TH,SD}}$ is the heat loss over the storage surface. As η_{C}, η_{D}, ϵ_{COP}, $R_{\mathrm{B,SD}}$ and $R_{\mathrm{TH,SD}}$ vary depending on input power and storage states in the simulation models, they need to be approximated for the optimization. This was done by calculating the average values of those variables from the look-up tables described in Section 2.

The electrical power balance is:

$$P_{\mathrm{PV}}(k) - P_{\mathrm{L}}(k) = P_{\mathrm{B,C}}(k) - P_{\mathrm{B,D}}(k) + P_{\mathrm{HP}}(k) + P_{\mathrm{PV,ct}}(k) + P_{\mathrm{G,FI}}(k) - P_{\mathrm{G,B}}(k) \; \forall k. \tag{18}$$

In addition to the energy balances, Equation (16) through Equation (18), and the inequality Constraints (12), (13) and (15), three more inequality constraints are needed in order to exclude the physically impossible decision of charging and discharging the battery simultaneously:

$$P_{\mathrm{B,C}}(k) \leq s_{\mathrm{B,C}}(k) \cdot P_{\mathrm{B,C,max}} \; \forall k, \tag{19}$$

$$P_{\mathrm{B,D}}(k) \leq s_{\mathrm{B,D}}(k) \cdot P_{\mathrm{B,D,max}} \; \forall k, \tag{20}$$

$$s_{\mathrm{B,C}}(k) + s_{\mathrm{B,D}}(k) \leq 1 \; \forall k, \tag{21}$$

where $s_{\mathrm{B,C}}$ and $s_{\mathrm{B,D}}$ are binary variables identifying the decision whether to charge or discharge the battery in the respective time step. The restriction of the heat pump either being switched off or switched on with a power higher than 20% of the nominal value is implemented in a similar way:

$$P_{\mathrm{HP}}(k) \geq s_{\mathrm{HP}}(k) \cdot P_{\mathrm{HP,min}} \; \forall k, \tag{22}$$

$$P_{\mathrm{HP}}(k) \leq s_{\mathrm{HP}}(k) \cdot P_{\mathrm{HP,max}} \; \forall k. \tag{23}$$

Furthermore, the values the variables can take need to be limited, either for physical or for legal reasons (e.g., the feed-in limit in Germany is half the PV generator's nominal power, if a certain government subsidy is used). These limits mostly depend on the data of the specific equipment which is used. The limits used in this investigation are shown in Table 1.

4. Investigations and Results

The aim of the simulation-based investigations in this paper is to:

1. Demonstrate the viability of the MILP-based MPC approach for the energy management of a hybrid energy storage system consisting of a PV plant, a battery and a combined heat pump/heat storage device,
2. Compare the performance of this concept to that of a simple rule-based strategy, and
3. Identify improvement potentials for the MPC of the described hybrid energy storage system.

First, the model parameters and the evaluation criteria are shortly presented. Then, the MPC-based energy management concept is compared qualitatively to the self-consumption strategy by analyzing the power and storage state trajectories on some example days. Afterwards a quantitative comparison allowing to generalize the qualitative results is drawn. Finally, the improvement potential of the new scheme is assessed by comparing its performance using real and ideal forecasts.

4.1. Model Parameters

There are several sets of parameters that need to be specified. The time series of electric load and PV power have been scaled to annual energy consumptions/productions of 4 MWh and 5 MWh,

respectively. In this case, this implies a 5.9 kW PV plant. The heat needed for DHW production amounts to about 2.5 MWh. The simulations have been carried out with one-minute time steps.

Table 1. Limits of the optimization variables.

Variable	Lower Limit	Upper Limit	Variable	Lower Limit	Upper Limit
E_{B}	0 kWh	5 kWh	$P_{\mathrm{ct}}(k)$	0 kW	$P_{\mathrm{PV}}(k)$
$P_{\mathrm{B,c}}$	0 kW	5 kW	U	$-\infty$	5.23 kWh
$P_{\mathrm{B,d}}$	0 kW	5 kW	P_{HP}	0 kW	0.85 kW
$P_{\mathrm{G,B}}$	0 kW	∞	$s_{\mathrm{B,c}}$	0	1
$P_{\mathrm{G,B,max}}$	0 kW	∞	$s_{\mathrm{B,d}}$	0	1
$P_{\mathrm{G,FI}}$	0 kW	2.95 kW	s_{HP}	0	1
$P_{\mathrm{G,FI,max}}$	0 kW	∞	U_{penalty}	0	∞

As can be seen from Table 1, the battery has a usable capacity of 5 kWh and maximum charging and discharging powers of 5 kW. The air-source heat pump for DHW production has a nominal power of 0.85 kW. At full load it has a COP of 3.8 and at 20% part load it increases to 4.1. For the purpose of calculating the heat supplied by the heat pump, the cold water supply is assumed to be at 10 °C. The 300 l heat storage has a maximum temperature of 60 °C, with the reference temperature set to $T_{\mathrm{ref}} = 45\,^{\circ}\mathrm{C}$ resulting in a capacity of 5.23 kWh. The ambient temperature used for heat storage self-discharge calculation is $T_{\mathrm{a}} = 20\,^{\circ}\mathrm{C}$. The U_{min} parameter from Constraint (9) is set to a value corresponding to 50 °C in order to avoid health risks because of legionella.

Prior to this investigation, a sensitivity analysis has been carried out in order to appropriately choose the prediction horizon, adaptation interval and the objective function parameters α, β, and γ in relation to the energy costs. As a result, the adaptation interval is set to 30 min and the prediction horizon K is 36 time steps (18 h). The electricity price is assumed to be 0.30 $\frac{€}{\mathrm{kWh}}$ and the feed-in remuneration is 0.12 $\frac{€}{\mathrm{kWh}}$. Both values are close to the current prices in Germany. The objective function parameters α and β are set to $0.1 \times \frac{K \cdot \Delta t}{8}$ in order to give the peak-shaving terms a similar weight as those for cost reduction. γ has a much higher value of 10 because it models a constraint (sufficiently high water temperature) that should be met before trying to reduce costs or peak powers.

4.2. Evaluation Criteria

For the evaluation of the simulations, several criteria were used. Because of the system being used for self-consumption, first the degree of self-sufficiency:

$$k_{\mathrm{ss}} = \frac{\int_{t=0}^{8760\ \mathrm{h}} \left(P_{\mathrm{L}}(t) + P_{\mathrm{HP}}(t) - P_{\mathrm{G,B}}(t)\right)\,\mathrm{d}t}{\int_{t=0}^{8760\ \mathrm{h}} \left(P_{\mathrm{L}}(t) + P_{\mathrm{HP}}(t)\right)\,\mathrm{d}t}, \tag{24}$$

and the degree of self-consumption:

$$k_{\mathrm{sc}} = \frac{\int_{t=0}^{8760\ \mathrm{h}} \left(P_{\mathrm{PV}}(t) - P_{\mathrm{G,FI}}(t)\right)\,\mathrm{d}t}{\int_{t=0}^{8760\ \mathrm{h}} P_{\mathrm{PV}}(t)\,\mathrm{d}t}, \tag{25}$$

as well as total operating costs C should be evaluated (compare [4,11,25]).

The static feed-in limit of 50% of the nominal PV power combined with the PV time series used for this study always leads to the maximum feed-in sometime during the year being exactly this value. However, the feed-in peak-shaving performance can be evaluated by examining the share of the potential PV energy, that had to be curtailed [11]:

$$k_{\mathrm{ct}} = \frac{\int_{t=0}^{8760\ \mathrm{h}} P_{\mathrm{PV,ct}}(t)\,\mathrm{d}t}{\int_{t=0}^{8760\ \mathrm{h}} P_{\mathrm{PV}}(t)\,\mathrm{d}t}. \tag{26}$$

The demand peak-shaving performance is evaluated by calculating a grid-relief factor $k_{g,99}$, defined as:

$$k_{g,99} = 1 - \frac{\pi_{99}(P_{G,B}(t))}{\pi_{99}(P_L(t) + P_{HP}(t))}, \tag{27}$$

where $\pi_{99}(P_i)$ denotes the 99th percentile of the respective power time series. The use of the 99th percentile instead of a maximum compensates for the possibility that the MPC scheme may fail to keep the battery sufficiently charged for only a very short time in between two optimization steps because of wrong forecasts. These short time intervals should not present a problem because between several homes that could employ this control scheme, they should not occur simultaneously. If the MPC-based control fails for a longer time, this would still be seen in this evaluation criterion.

For the purpose of evaluation, it is considered sufficient for the DHW drawn by the consumer to have a temperature of 45 °C. Therefore, DHW availability k_{DHW} is defined as:

$$k_{DHW} = \frac{\int \dot{V}_{DHW}\big|_{T_{HS} \geq 45\ °C}(t)\ \mathrm{d}t}{\int \dot{V}_{DHW}(t)\ \mathrm{d}t}. \tag{28}$$

As the MPC-based peak-shaving control uses the battery and the heat storage in a different way than a simple rule-based operating scheme, the dwelling time of the battery at high and low SOCs, battery full cycles k_{fc}, the annual efficiency of the battery and the inverter ϵ_B and the ratio of the used heat to the electrical energy used by the heat pump ϵ_{HP}, which is similar but not identical to the annual COP, are evaluated as well:

$$k_{fc} = \frac{\int P_{B,c}(t) + P_{B,d}(t)\ \mathrm{d}t}{2 \cdot E_{B,max}}, \tag{29}$$

$$\epsilon_B = 1 - \frac{\int P_{B,c}(t) - P_{B,d}(t)\ \mathrm{d}t}{\int P_{B,c}(t)\ \mathrm{d}t}, \tag{30}$$

$$\epsilon_{HP} = \frac{\int \dot{Q}_{DHW}(t)\ \mathrm{d}t}{\int P_{HP}(t)\ \mathrm{d}t}. \tag{31}$$

4.3. Qualitative Comparison

As described in Section 3, the MPC aims to reduce grid power peaks additionally to reducing cost. Therefore, the control scheme uses both storage units differently than a simple rule-based self-consumption scheme. In this case, the self-consumption scheme has been implemented based on three rules: firstly, if the heat storage temperature is below 50 °C, the heat pump has to operate at full power in order to raise the heat storage temperature, regardless if there is excess PV power. Secondly, if there is excess PV power, it should be used for heat storage charging. Only if there is still excess PV power, it is used for battery charging. The remaining excess PV power is either exported to the grid or curtailed. The battery is immediately discharged if the load is higher than the supply.

Figure 4a shows the PV and load powers, Figure 4b the grid powers (feed-in positive) and Figure 4c the battery SOCs for the self-consumption scheme, the MPC scheme with real forecasts, and the MPC scheme with ideal forecasts during a period of three days at the end of June of the simulated year. Firstly, comparing the rule-based scheme to both MPC variants in Figure 4c, one can see that the MPC scheme usually starts charging the battery later during the day, instead starting early to feed the power into the grid which can be seen in Figure 4b. In the ideal case, the battery is still fully charged at the end of the day, whereas with real forecasts there are of course days (here: the second day) when this does not work out perfectly.

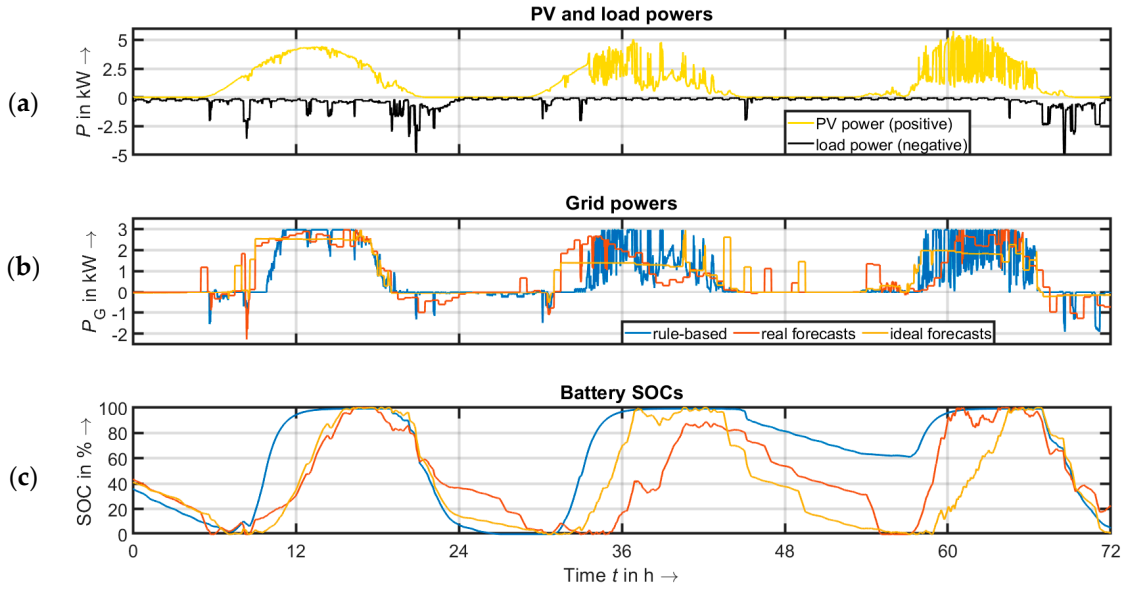

Figure 4. Comparison of grid powers and battery use. (**a**) PV and load powers. (**b**) Grid powers. (**c**) Battery SOCs.

On the second and third days, there seem to have been a lot of small clouds in the sky, causing the PV power to fluctuate heavily as can be seen from Figure 4a. With the battery fully charged, the rule-based approach cannot compensate for this, thus, the grid power in Figure 4b fluctuates heavily as well. The MPC-based scheme, however, uses the battery to compensate for these fluctuations. The power steps that can still be seen in those two time series happen on a larger time scale (30 min, not 1 min), and can therefore be considered less problematic.

While the previously described effects are intended, there are also some interesting side-effects. Firstly, because of the MPC concept delaying the battery charging, the battery spends less time at high SOCs, which is considered a major factor in the degradation of lithium-ion batteries. The extent of this effect can be seen in the duration curves of the Battery SOC obtained from the one-year simulation in Figure 5. Secondly, the battery is charged with less power (less steep SOC trajectory). Because of the nonlinear dependency of losses from battery current, this reduces the losses per energy throughput and probably ageing as well.

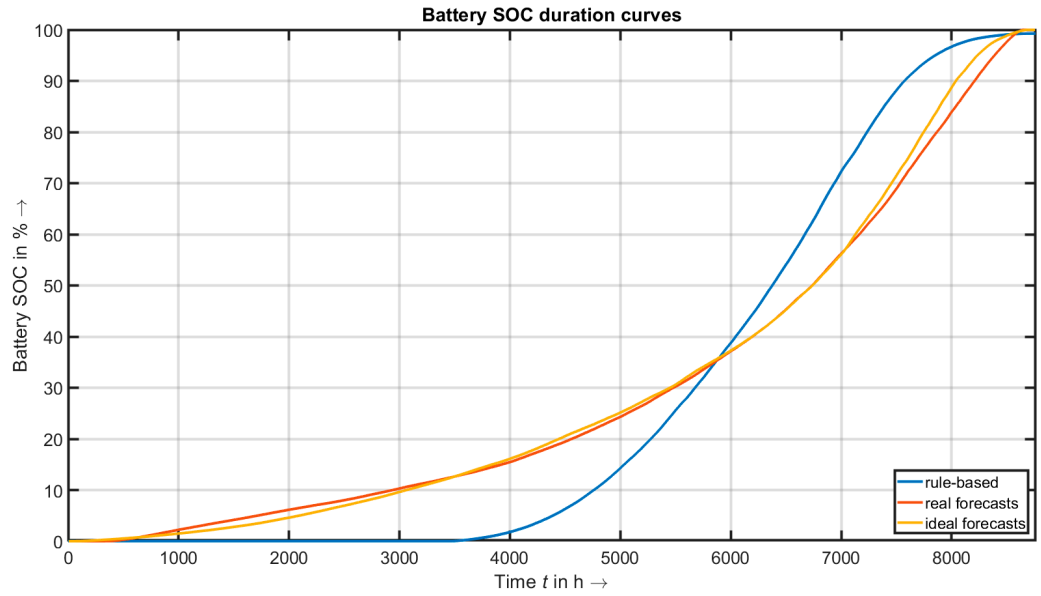

Figure 5. Battery SOC duration curves.

However, using the battery to compensate for fluctuations also means that the energy throughput is higher (see the "microcycles", especially on the second and third day), which may counter the previously found benefits concerning ageing and losses.

Figure 6b shows the heat pump powers and Figure 6c the average heat storage temperatures for one day at the beginning of April. It can be seen that both strategies try to use the heat pump whenever there is a PV surplus, which can be seen in Figure 6a, especially between about 1 and 5 p.m. on the example day. However, very often the heat storage self-discharge and an early DHW demand lead to the heat storage being completely discharged in the morning in the case of the self-consumption strategy (seen here at about 6 a.m.). Combined with the first rule of said strategy, this leads to part of the daily heat storage charging being done before enough PV power is available. Afterwards, the storage is full which is why the strategy actually does not reach the best degrees of self-consumption and self-sufficiency possible.

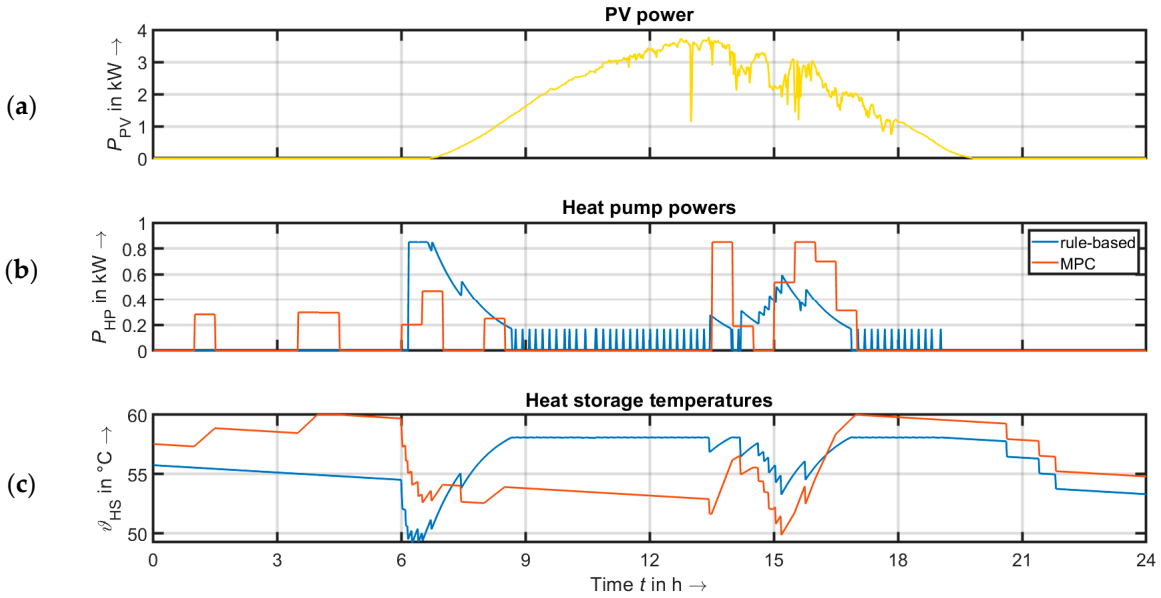

Figure 6. Comparison of heat pump usage. (**a**) PV power. (**b**) Heat pump power. (**c**) Heat storage temperatures.

The new MPC-based strategy, on the other hand, partly charges the heat storage during the night and leaves it at lower temperature in the morning, allowing for more of the surplus PV being charged into the heat storage later on. This shows the potential of an MPC-based strategy for intelligent demand-side management using the heat pump. This potential could be increased if further flexible loads were to be included in the system.

4.4. Quantitative Comparison

Table 2 shows the results of the simulations of both, the new MPC-based control scheme and the rule-based scheme, over one year with respect to the previously introduced evaluation criteria.

One can see that the peak-shaving strategy successfully reduces curtailment and grid demand peaks compared to the rule-based strategy while reaching approximately the same DHW availability. However, these positive results are bought by reducing self-sufficiency and self-consumption, and therefore, increasing operation costs.

Additionally, the battery is used more, which increases full cycles and therefore ageing. With the number of full cycles increasing considerably, the absolute losses inside the battery and its inverter also increase, but put in relation to the battery's energy throughput, losses are significantly lower. This shows the positive side-effect, namely the grid power smoothing implicitly meaning lower average battery powers and therefore reduced losses, mentioned in Section 4.3. Note that a large part of the absolute losses (about 100 kWh) is made up of self-discharge and the battery management system, meaning that it cannot be reduced by any energy management strategy.

Table 2. Results of real and ideal dynamic peak-shaving compared to rule-based self-consumption strategy.

Criterion	Rule-Based Self-Consumption	Mpc-Based, Real Forecasts	Mpc-Based, Ideal Forecasts
k_{ss}	51.7%	47.8%	53.4%
k_{sc}	59.9%	57.1%	62.0%
k_{ct}	2.50%	0.25%	0.03%
$k_{g,99}$	18.8%	33.2%	64.3%
k_{DHW}	97.9%	97.8%	100.0%
C	462 €	498 €	445 €
k_{fc}	240	399	382
ϵ_B	68.9%	76.1%	75.6%
ϵ_{HP}	3.16	3.09	3.13

While the reduction of grid power peaks offers a great potential for reducing infrastructure cost for the whole society, the trade-offs of this strategy will very probably prevent PV battery system owners from adopting such a strategy within the current regulation in Europe. Therefore, policy-makers should offer or enable financial incentives compensating the lower self-sufficiency and a possibly lower battery lifetime, in order to encourage them to adopt such a peak shaving strategy.

4.5. Improvement Potentials

In order to assess improvement potentials for the MPC-based double peak-shaving, the simulations have also been run with ideal forecasts. The results are shown in Table 2 as well.

With ideal forecasts, curtailment, grid relief and DHW availability are improved even further, while self-sufficiency, self-consumption and operation costs improve to values even better than those of the rule-based strategy. This is possible due to the suboptimal heat pump behavior explained in Section 4.3.

Figure 7a shows the duration curves for grid power achieved by the rule-based strategy and MPC scheme with real and ideal forecasts. It can be seen that on the feed-in side, detailed in Figure 7c, the MPC scheme with real forecasts reaches almost the same grid power smoothing that the MPC scheme with ideal forecasts does. However, on the demand side, detailed in Figure 7b, the MPC scheme with real forecasts does not perform much better than the rule-based strategy, although the results with ideal forecasts indicate a huge unused improvement potential.

These results indicate that by improving forecasts or explicitly taking into account forecast uncertainties in the problem formulation, further improvements of the peak shaving strategy's real performance are possible. Furthermore, while all other values improved when using ideal forecasts, the ϵ_B value got worse. Although this behavior may just be due to there being less full cycles or the higher losses being necessary in order to achieve the other improvements, it raises the question whether taking the nonlinear battery behavior into account in the optimization formulation (e.g., by using a nonlinear programming technique) may reduce losses even further.

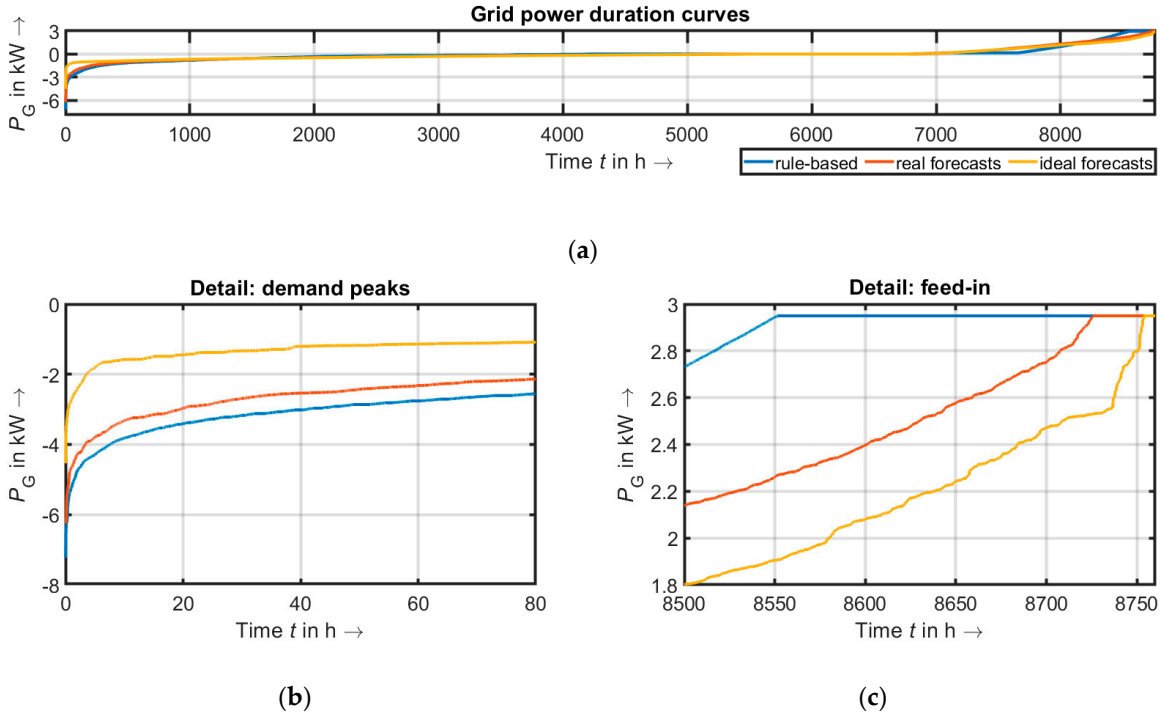

Figure 7. Grid power duration curves. (**a**) Duration curves. (**b**) Detail: demand peaks. (**c**) Detail: feed-in.

5. Conclusions

The results prove that the energy management concept described in Section 3 is able to fulfill its objectives. While economic performance in the current legislative situation of Germany is slightly worse than that of a rule-based self-consumption strategy, it successfully reduces grid power peaks, therefore offering a potential for infrastructure cost reduction if adopted by a large amount of prosumers. Furthermore, it leads to the battery spending less time at high SOCs and being charged with lower powers which can be considered beneficial to its lifetime.

Potentials for further improvements have been identified in two areas. Firstly, there is a large gap between the performances of the energy management with real forecasts and with ideal forecasts. Therefore, performance may be improved considerably by improving forecasts and taking into account the uncertainties related to the stochastic behavior of PV and load powers.

Secondly, the linearization of the battery and heat pump loss characteristics in the optimization problem formulation leads to the optimization solver not seeing any difference in using the devices for a short period of time with high power or a longer period of time with less power. The latter, however, would lead to a higher efficiency. Therefore, there may be some improvement potential in modeling this nonlinear behavior in the optimization problem formulation.

Future work will therefore focus on using these improvement potentials. Furthermore, the effects of the increased number of battery full cycles at lower powers on ageing will be analyzed and other applications of the energy management strategy may be investigated. This includes the introduction of more demanding but flexible loads, such as electric water heaters or electric vehicles, and the coordination of several of these prosumers and evaluation of their combined performance in relieving the grid.

Author Contributions: Conceptualization, R.G. and T.B.; methodology, R.G., M.B., and T.B.; software, R.G. and M.B.; validation, R.G. and M.B.; formal analysis, R.G.; investigation, R.G.; resources, T.B.; data curation, R.G., M.B. and T.B.; writing—original draft preparation, R.G.; writing—review and editing, R.G., M.B., and T.B.; visualization, R.G.; supervision, T.B.; project administration, T.B.; funding acquisition, T.B.

Funding: This research received no external funding.

Conflicts of Interest: The authors declare no conflict of interest.

Nomenclature

Abbreviations	
COP	coefficient of performance
DHW	domestic hot water
MILP	mixed-integer linear programming
MPC	model predictive control
PV	photovoltaics
SOC	state of charge
Indices and sets	
k	index of time step
t	current time (continuous)
MPC and objective function parameters	
α	relative weight of grid import power smoothing/reduction
β	relative weight of grid export power smoothing/reduction
γ	relative weight of penalty for heat storage deep discharge
Δt	time step size
K	number of time steps in prediction horizon
Evaluation criteria	
ϵ_{B}	annual battery efficiency
ϵ_{HP}	annual heat pump and heat storage efficiency
π_{99}	99th percentile of a time series
k_{ct}	percentage of potential PV energy that had to be curtailed
k_{DHW}	DHW availability
k_{fc}	number of equivalent battery full cycles
$k_{\mathrm{g},99}$	grid relief factor
k_{sc}	degree of self-consumption
k_{ss}	degree of self-sufficiency
Variables	
ϵ_{COP}	average heat pump COP
η_{C}	average battery and inverter charging efficiency
η_{D}	average battery and inverter discharging efficiency
A	heat storage surface
C	operation cost of the hybrid energy storage system
E_{B}	battery energy content
F	objective function
F_{thermal}	penalty term for thermal discomfort
P_{B}	total battery inverter AC power
$P_{\mathrm{B,C}}$	battery inverter charging power
$P_{\mathrm{B,C,max}}$	rated battery inverter charging power
$P_{\mathrm{B,D}}$	battery inverter discharging power
$P_{\mathrm{B,D,max}}$	rated battery inverter discharging power
$P_{\mathrm{B,L}}$	total battery and inverter losses
P_{G}	grid power
$P_{\mathrm{G,B}}$	grid import (bought) power
$P_{\mathrm{G,B,max}}$	maximum grid import power in prediction horizon
$P_{\mathrm{G,FI}}$	grid feed-in (sold) power
$P_{\mathrm{G,FI,max}}$	maximum grid feed-in power in prediction horizon
$P_{\mathrm{G,max}}$	legal grid feed-in power limit
P_{HP}	heat pump power
P_{L}	load power
$P_{\mathrm{L,f}}$	forecasted load power
P_{PV}	possible PV power (from measured time series)
$P_{\mathrm{PV,ct}}$	curtailed PV power
$P_{\mathrm{PV,env}}$	envelope of the PV power of preceding days

$\dot{Q}_{\mathrm{DHW}}$	enthalpy flow of the hot water being drawn
$\dot{Q}_{\mathrm{HP}}$	heat pump thermal power
$R_{\mathrm{B,SD}}$	battery self-discharge rate
$R_{\mathrm{TH,SD}}$	thermal storage self-discharge rate
T_{HS}	heat storage temperature
T_{a}	ambient temperature
T_{ref}	reference temperature for heat storage enthalpy
U	heat storage enthalpy
U_{min}	desired minimum heat storage enthalpy
U_{penalty}	amount by which enthalpy is lower than the desired minimum
$\dot{V}_{\mathrm{DHW}}$	volume flow of hot water being drawn
c_p	specific heat capacity
k_{th}	heat transmittance
$m_{\mathrm{H_2O}}$	mass of water in the heat storage
$p_{\mathrm{G,B}}$	electricity price
$p_{\mathrm{G,FI}}$	feed-in remuneration
$s_{\mathrm{B,C}}$	decision to charge the battery
$s_{\mathrm{B,D}}$	decision to discharge the battery
s_{HP}	decision to switch on the heat pump

References

1. The International Renewable Energy Agency (IRENA). Renewable Energy Statistics 2018. Abu Dhabi. 2018. Available online: https://www.irena.org/publications/2018/Jul/Renewable-Energy-Statistics-2018 (accessed on 16 April 2019).
2. Kondziella, H.; Bruckner, T. Flexibility requirements of renewable energy based electricity systems—A review of research results and methodologies. *Renew. Sustain. Energy Rev.* **2016**, *53*, 10–22. [CrossRef]
3. Ashouri, A.; Fux, S.S.; Benz, M.J.; Guzzella, L. Optimal design and operation of building services using mixed-integer linear programming techniques. *Energy* **2013**, *59*, 365–376. [CrossRef]
4. Williams, C.J.; Binder, J.O.; Kelm, T. Demand side management through heat pumps, thermal storage and battery storage to increase local self-consumption and grid compatibility of PV systems. In Proceedings of the IEEE PES Innovative Smart Grid Technologies Europe 2012, Berlin, Germany, 14–17 October 2012. [CrossRef]
5. Kuboth, S.; Heberle, F.; König-Haagen, A.; Brüggemann, D. Economic model predictive control of combined thermal and electric residential building energy systems. *Appl. Energy* **2019**, *240*, 372–385. [CrossRef]
6. Halvgaard, R.; Poulsen, N.K.; Madsen, H.; Jørgensen, J.B. Economic model predictive control for building climate control in a smart grid. In Proceedings of the IEEE PES Innovative Smart Grid Technologies (ISGT) 2012, Washington, DC, USA, 16–18 January 2012. [CrossRef]
7. Bocklisch, T. Hybrid energy storage approach for renewable energy applications. *J. Energy Storage* **2016**, *8*, 311–319. [CrossRef]
8. Paulitschke, M.; Bocklisch, T.; Böttiger, M. Comparison of particle swarm and genetic algorithm based design algorithms for PV-hybrid systems with battery and hydrogen storage path. *Energy Procedia* **2017**, *135*, 452–463. [CrossRef]
9. Weyers, C.; Bocklisch, T. Simulation-based investigation of energy management concepts for fuel cell-battery-hybrid energy storage systems in mobile applications. *Energy Procedia* **2018**, *155*, 295–308. [CrossRef]
10. Angenendt, G.; Zurmühlen, S.; Mir-Montazeri, R.; Magnor, D.; Sauer, D.U. Enhancing Battery Lifetime in PV Battery Home Storage System Using Forecast Based Operating Strategies. *Energy Procedia* **2016**, *99*, 80–88. [CrossRef]
11. Bergner, J.; Weniger, J.; Tjaden, T.; Quaschning, V. Feed-in Power Limitation of Grid-Connected PV Battery Systems with Autonomous Forecast-Based Operation Strategies. In Proceedings of the 29th European PV Solar Energy Conference and Exhibition, Amsterdam, The Netherlands, 22–26 September 2014. [CrossRef]

12. Kanchev, H.; Lu, D.; Colas, F.; Lazarov, V.; Francois, B. Energy Management and Operational Planning of a Microgrid with a PV-Based Active Generator for Smart Grid Applications. *IEEE Trans. Ind. Electron.* **2011**, *58*, 4583–4592. [CrossRef]
13. Psimopoulos, E.; Bee, E.; Luthander, R.; Bales, C. Smart Control Strategy for PV and Heat Pump System Utilizing Thermal and Electrical Storage and Forecast Services. In Proceedings of the joint Solar World Congress and International Conference on Solar Heating and Cooling for Buildings and Industry SWC2017/SHC2017, Abu Dhabi, UAE, 29 October–2 November 2017. [CrossRef]
14. Bee, E.; Prada, A.; Baggio, P. Demand-Side Management of Air-Source Heat Pump and Photovoltaic Systems for Heating Applications in the Italian Context. *Environments* **2018**, *5*, 132. [CrossRef]
15. Keerthisinghe, C.; Chapman, A.C.; Verbič, G. Energy Management of PV-Storage Systems: Policy Approximations Using Machine Learning. *IEEE Trans. Ind. Inf.* **2019**, *15*, 257–265. [CrossRef]
16. Rahbar, K.; Xu, J.; Zhang, R. Real-Time Energy Storage Management for Renewable Integration in Microgrid: An Off-Line Optimization Approach. *IEEE Trans. Smart Grid* **2015**, *6*, 124–134. [CrossRef]
17. Maleki, A.; Rosen, M.; Pourfayaz, F. Optimal Operation of a Grid-Connected Hybrid Renewable Energy System for Residential Applications. *Sustainability* **2017**, *9*, 1314. [CrossRef]
18. Pedrasa, M.A.A.; Spooner, T.D.; MacGill, I.F. Coordinated Scheduling of Residential Distributed Energy Resources to Optimize Smart Home Energy Services. *IEEE Trans. Smart Grid* **2010**, *1*, 134–143. [CrossRef]
19. Wu, Z.; Tazvinga, H.; Xia, X. Demand side management of photovoltaic-battery hybrid system. *Appl. Energy* **2015**, *148*, 294–304. [CrossRef]
20. Parisio, A.; Rikos, E.; Glielmo, L. Stochastic model predictive control for economic/environmental operation management of microgrids: An experimental case study. *J. Process Control* **2016**, *43*, 24–37. [CrossRef]
21. Keerthisinghe, C.; Verbič, G.; Chapman, A.C. Evaluation of a multi-stage stochastic optimization framework for energy management of residential PV-storage systems. In Proceedings of the Australasian Universities Power Engineering Conference, AUPEC 2014, Perth, Australia, 28 September–1 October 2014. [CrossRef]
22. Powell, W.B.; Meisel, S. Tutorial on Stochastic Optimization in Energy—Part I: Modeling and Policies. *IEEE Trans. Power Sys.* **2016**, *31*, 1459–1467. [CrossRef]
23. Romero-Quete, D.; Rosero Garcia, J. An affine arithmetic-model predictive control approach for optimal economic dispatch of combined heat and power microgrids. *Appl. Energy* **2019**, *242*, 1436–1447. [CrossRef]
24. Keerthisinghe, C.; Verbič, G.; Chapman, A.C. Energy management of PV-storage systems: ADP approach with temporal difference learning. In Proceedings of the 2016 Power Systems Computation Conference (PSCC), Genoa, Italy, 20–24 June 2016. [CrossRef]
25. Böttiger, M.; Paulitschke, M.; Bocklisch, T. Innovative Reactive Energy Management for a Photovoltaic Battery System. *Energy Procedia* **2016**, *99*, 341–349. [CrossRef]
26. Gelleschus, R.; Böttiger, M.; Stange, P.; Bocklisch, T. Comparison of optimization solvers in the model predictive control of a PV-battery-heat pump system. *Energy Procedia* **2018**, *155*, 524–535. [CrossRef]
27. Böttiger, M.; Paulitschke, M.; Bocklisch, T. Systematic experimental pulse test investigation for parameter identification of an equivalent circuit based lithium-ion battery model. *Energy Procedia* **2017**, *135*, 337–346. [CrossRef]
28. Heo, J.; Jeong, M.W.; Kim, Y. Effects of flash tank vapor injection on the heating performance of an inverter-driven heat pump for cold regions. *Int. J. Refrig.* **2010**, *33*, 848–855. [CrossRef]
29. Jordan, U.; Vajen, K. DHWcalc: Program to generate domestic hot water profiles with statistical means for user defined conditions. In Proceedings of the Solar World Congress 2005, Orlando, FL, USA, 6–12 August 2005; pp. 1525–1530, ISBN 978-1-622762-63-7.
30. Bergner, J.; Weniger, J.; Tjaden, T.; Quaschning, V. Verbesserte Netzintegration von PV-Speichersystemen durch Einbindung lokal erstellter PV- und Lastprognosen. In Proceedings of the 30. Symposium Photovoltaische Solarenergie, Kloster Banz, Bad Staffelstein, Germany, 4–6 March 2015; ISBN 978-3-943891-45-4.

© 2019 by the authors. Licensee MDPI, Basel, Switzerland. This article is an open access article distributed under the terms and conditions of the Creative Commons Attribution (CC BY) license (http://creativecommons.org/licenses/by/4.0/).